

A Novel Redox Indicator based on Relative Abundances of C₃₁ And C₃₂ Homohopanes in the Eocene Lacustrine Dongying Depression, East China

Chong Jiang

China University of Geosciences (Beijing)

Haiping Huang (✉ huah@ucalgary.ca)

China University of Geosciences (Beijing)

Zheng Li

Geology Scientific Research Institute of Shengli Oilfield Company

Hong Zhang

Yangtze University

Zheng Zhai

Geology Scientific Research Institute of Shengli Oilfield Company

Research Article

Keywords: Shahejie Formation (Es), Dongying Depression, redox conditions, pentacyclic terpanes, homohopane index (HHI), gammacerane index (G/C_{30H}).

Posted Date: April 14th, 2021

DOI: <https://doi.org/10.21203/rs.3.rs-396664/v1>

License:  This work is licensed under a Creative Commons Attribution 4.0 International License. [Read Full License](#)

Version of Record: A version of this preprint was published at Petroleum Science on February 1st, 2022. See the published version at <https://doi.org/10.1016/j.petsci.2022.01.019>.

Abstract

A suite of oils and bitumens from the Eocene Shahejie Formation (Es) in the Dongying Depression, East China was geochemically characterized to illustrate the impact of source input and redox conditions on the distributions of pentacyclic terpanes. The fourth member (Es4) developed under highly reducing, sulfidic hypersaline conditions, while the third member (Es3) formed under dysoxic, brackish to freshwater conditions. Oils derived from Es4 are enriched in C_{32} homohopanes ($C_{32}H$), while those from Es3 are prominently enriched in C_{31} homohopanes ($C_{31}H$). The $C_{32}H/C_{31}H$ ratio shows positive correlation with homohopane index (HHI), gammacerane index ($G/C_{30}H$), and negative correlation with pristane/phytane (Pr/Ph) ratio, and can be used to evaluate oxic/anoxic conditions during deposition and diagenesis. High $C_{32}H/C_{31}H$ ratio (> 0.8) is an important characteristic of oils derived from sulfidic, hypersaline anoxic environments, while low values (< 0.8) indicate non-sulfidic, dysoxic conditions. Extremely low $C_{32}H/C_{31}H$ ratios (< 0.4) indicate strong oxic conditions of coal deposition. Advantages to use $C_{32}H/C_{31}H$ ratio as redox condition proxy compared to the HHI and gammacerane indexes are wider valid maturity range, less sensitive to biodegradation influence and better differentiation of reducing from oxic environments. Preferential cracking of C_{35} -homohopanes leads HHI to be valid in a narrow maturity range before peak oil generation. No C_{35} homohopane can be reliably detected in the Es4 bitumens when vitrinite reflectance is $> 0.75\%$, which explains the rare occurrence of high HHI values in Es4 source rocks. Gammacerane is thermally more stable and biologically more refractory than C_{30} hopane, leading $G/C_{30}H$ ratio more sensitive to maturation and biodegradation than $C_{32}H/C_{31}H$ ratio. Meanwhile, both HHI and gammacerane index cannot differentiate level of oxidation. The $C_{32}H/C_{31}H$ ratio can be applied globally as a novel redox proxy in addition to the Dongying Depression.

1. Introduction

Numerous biomarker parameters are available in the literature to diagnose organic facies and depositional environments. The *n*-alkane distribution [1], ratio of pristane (Pr) to phytane (Ph) [2], relative abundances of C_{27} , C_{28} and C_{29} steranes [3], occurrence of 28,30-bisnorhopane [4], C_{30} tetracyclic polyprenoids [5] and C_{30} steranes [6], elevated gammacerane and C_{35} -homohopane abundance [7, 8], are commonly used indicators among many others. Hopane distributions, in particular, have been the focus of biomarker investigations for decades because of their ubiquitous occurrence in geological samples and their unique precursors in organisms and sensitivity to redox conditions at the time of sediment deposition [9]. Hopanes are primarily derived from biochemical processes in bacteria and cyanobacteria [10], and their diagenetic and catagenetic evolution after burial in sediments is relatively well understood [11, 12]. Origin, redox conditions, and thermal alteration are the three main factors controlling the final distributions of hopanes in the source rock extracts (bitumens) and related oils [9–11].

C_{29} 17 α ,21 β (H) 30-norhopane ($C_{29}H$) and C_{30} 17 α ,21 β (H) hopane ($C_{30}H$) are typically the most abundant hopane components in oils and bitumens. The relative abundance of $C_{29}H$ and $C_{30}H$ appears to be sensitive to lithological changes with $C_{29}H/C_{30}H$ ratios of > 1.0 characterizing evaporitic-anoxic carbonate source rocks, while lower values (< 1.0) indicates a clay-rich siliciclastic source [13]. Homohopanes ($C_{31}H$ – $C_{35}H$) are generally believed to originate from bacteriohopanepolyols, which are synthesized as membrane lipids by bacteria [10–12]. The C_{35} homohopanes are selectively preserved by sulfur incorporation under anoxic conditions, while lower carbon homologues are preferentially preserved under suboxic to oxic conditions due to side chain cleavage [12, 14–15]. Dominant C_{31} homohopanes without C_{34} and C_{35} homohopanes usually indicates terrigenous plant-derived organic matter, especially in coaly strata [16–17], while the dominance of C_{33} homohopane, coupled with the elevated 28,30-bisnorhopane ratio, may be indicative of specific bacterial input in an anoxic marine niche environment [18]. A commonly used indicator of depositional conditions of source rocks is the homohopane index [$HHI = C_{35}/\Sigma(C_{31} - C_{35}) (22S + 22R)$] [8]. Bishop and Farrimond [19] further proposed that a $C_{31}H:C_{33}H:C_{35}H$ ternary diagram, coupled with a hopane odd/even predominance parameter, is a good depiction of overall homohopane carbon number distributions. They applied the distributions of homohopanes for oil-oil and oil-source rock correlation in the North Sea. However, the causes of homohopane compositional differences and their significance in geochemical application remain poorly understood.

Generally, oils and bitumens derived from highly reducing environments of deposition contain high relative abundance of C_{32} – C_{35} homohopanes, while those from freshwater lacustrine environments have low abundance of homohopanes, especially C_{33} – C_{35} homohopanes [20–21]. The preservation of distinctive carbon numbers of extended hopanes appears to be controlled by the availability of free oxygen during deposition [7]. For example, the marine Triassic Filletino oil from the Adriatic Sea shows elevated C_{32} homohopane and gammacerane [22]. However, variations of the C_{32}/C_{31} homohopane ratio in geological samples and its application to assess depositional environment has not been fully explored.

The Dongying Depression in the Bohai Bay Basin, east China, is a prolific oil production province where the source rocks were deposited under variable conditions from strongly reducing, anoxic hypersaline water to relatively oxic freshwater during basin evolution. The geochemical features of source rocks and oils from this basin have been thoroughly investigated [23–26], and C_{32}/C_{31} homohopane ratios show a wide range of variation in oils and source rock extracted bitumens. The purpose of the present study is to explore the geochemical significance of the C_{32}/C_{31} homohopane ratio in the determination of redox conditions during deposition of source rocks, and the factors governing the C_{32}/C_{31} homohopane ratio during thermal maturation or alteration processes.

2. Geological Background

The Dongying Depression, with an area of approximately 5700 km², is a typical half-graben lacustrine depression situated in the southeast Jiyang Sub-basin, Bohai Bay Basin, East China (Fig. 1). It is an asymmetric depression with a steeply faulted zone in the northern side and a very gentle slope in the southern side. It is bounded by several structural highs and consists of the Lijin, Minfeng, Niuzhuang and Boxing sags and a central anticline. Detailed structural evolution, sediment deposition, and petroleum generation and accumulation in the depression have been well documented [27–31]. Briefly, sediments in the

Dongying Depression are mainly of Cenozoic age and can be divided into the Paleogene Kongdian (Ek), Eocene Shahejie (Es) and Dongying (Ed), the Neogene Guantao (Ng) and Minghuazhen (Nm) and the Quaternary Pingyuan formations. The Ek Formation was deposited unconformably on the Mesozoic and Paleozoic surface and is mainly composed of coarse clastic red beds with limited oil generation potential. The Es Formation is widely distributed and contains the most important source rocks and reservoirs in the basin. It can be further divided into four members, namely, Es1, Es2, Es3, and Es4 (from the youngest to the oldest). The Es4 Member formed under saline lacustrine conditions and is characterized by thick deposits of gypsum-halite, thin dolomites and oolitic limestones interbedded with calcareous shales, and organic-rich mudstones. The overlying Es3 Member was deposited in relatively deeper water under brackish to freshwater conditions. It consists mainly of gray and dark-gray mudstone, siltstone, and sandstone intercalated with brown–gray and gray-to-black shale (Fig. 1). Both members bear high oil and gas generation potential but oils derived from each member can be geochemically distinguished [23–31].

3. Methods

Oil samples were collected from 36 production wells with most samples situated at the southern slope of the Dongying Depression. Oils in shallow reservoir (< 1,500 m) suffered biodegradation [32], and severely biodegraded oils were excluded from the present study. Source rock samples were collected from three shale oil wells located in the Boxing (FY1), Niuzhuang (NY1) and Lijin (LY1) sags, respectively (Fig. 1). The core samples were pulverized to 80–100 mesh with a swing mill and then extracted using dichloromethane (DCM):methanol (MeOH) (93:7, v:v) for 72 h in a Soxhlet apparatus. Elemental sulfur was removed during the Soxhlet extraction using activated copper strips. The extractable organic matter (EOM) was determined using an in-house method. About 50 mg of EOM and/or oil was transferred to a vial and a suite of internal standards (cholestane-d₄, adamantane-d₁₆, phenyldodacane-d₃₀, naphthalene-d₈, phenanthrene-d₁₀ and 1,1-binaphthalene) was added, after which the sample was transferred to a polar Florisil solid phase extraction (SPE) cartridge to remove polar compounds and obtain the hydrocarbon fraction. The hydrocarbon fraction was further separated into the aromatic and saturated hydrocarbon fractions using a modified Bastow method [33]. In order to assure accuracy, a blank and two well characterized produced oils (a heavy oil and a light oil) were processed with each batch of samples in the same way as the rock extracts.

The saturated hydrocarbon fraction was analyzed using GC–MS in both selected ion monitoring and full-scan mode (SIM/SCAN) on an Agilent 7890B gas chromatograph linked to an Agilent 5977A MSD system. A DB–1MS fused silica capillary column (60 m × 0.32 mm i.d. × 0.25 μm film thickness) was used for separation. The GC oven temperature was programmed from 50°C (1 min) to 120°C at 20°C/min, then increased to 310°C at 3°C/min, which was held for 25 min. Helium was used as the carrier gas and a constant flow rate of 1 ml/min was applied. The temperature of the injector and interface was set at 300°C. The ion source was operated in the electron ionization (EI) mode at 70 eV. Peak identification was performed by comparisons of the retention time index and an MS standard library. Concentrations were calculated based on peak area and no response factor calibration was performed.

4. Results

4.1. Terpane distributions in oils and source rock extracts

The *m/z* 191 mass fragmentograms of representative oil samples in the saturated hydrocarbon fraction exhibit high proportions of pentacyclic terpanes (PT) relative to tricyclic terpanes (TT) (Fig. 2). The distributions of pentacyclic terpanes in all samples are dominated by C₃₀H with a general depletion from C₃₁ to C₃₅ homohopanes. Minor amounts of 18α(H)-trisorneohopane (Ts), 17α(H)-trisorhopane (Tm), C₂₉ and C₃₀ 17β, 21α(H) hopanes (moretananes), C₃₀ 17α (H)-diahopane (C₃₀D) and C₂₉ 18α(H)-30-norneohopane (C₂₉Ts) are also present. The main difference between Es3 and Es4 oils is the relative abundance of homohopanes and gammacerane. The Es3 oils are characterized by relatively low concentrations of gammacerane and little or no C₃₅ homohopane, showing a typical feature of freshwater lacustrine clastic source rocks. In contrast, the Es4 oils are enriched in gammacerane and relatively high levels of C₃₅ homohopane, suggesting hypersaline source rock deposition.

The *m/z* 191 chromatograms of saturated hydrocarbon fractions from representative source rock extracts exhibit very different features from the oils (Fig. 3). Only samples from wells FY1 and NY1 at relatively shallow depth bear the same features as oils from the Es3 and Es4 reservoirs, respectively, while deeply buried samples from well LY1 show drastically altered pentacyclic terpanes distribution patterns. The Es3 source rocks in the LY1 well show significantly depleted Tm and C₂₉H and relatively concentrated Ts, C₂₉Ts and C₃₀D, while homohopanes remain relatively constant; however, the Es4 source rocks show substantial depletion of C₂₉–C₃₅ regular hopanes with rearranged hopanes, especially Ts as a dominant peak. The C₃₄ and C₃₅ homohopanes are absent in a few of the deepest samples. Meanwhile, the abundance of tricyclic terpanes is relatively increased as compared to the pentacyclic terpanes (Fig. 3).

A few commonly used molecular parameters from the saturated hydrocarbon fraction in the studied samples are listed in Table 1. The C₃₂H/C₃₁H ratios vary from 0.59 to 0.96 with an average value of 0.72 in oils from the Es3 reservoir; while they range from 0.78 to 1.22 with an average value of 0.96 in oils from the Es4 reservoir (Table 1). While some overlap exists between the two reservoirs likely due to mixing of charge (some known mixed oils were excluded in this study), the systematic difference in C₃₂H/C₃₁H may reflect intrinsic differences in source rock depositional environment. However, the differences in bitumens are less obvious. High C₃₂H/C₃₁H ratios occur only in limited samples of the Es4 source rocks possibly due to thermal maturity influence. Figure 4 shows diagrams that compare the C₃₂H/C₃₁H ratio with other parameters that are sensitive to redox conditions. The homohopane index (HHI) values, expressed as the percent abundance of C₃₅ hopanes relative to the summed C₃₁ to C₃₅ hopane abundances [8], for the Es3 oils are in the range of 2.9–11.5% (average 6.3%) and those for the Es4 oils range from 7.6–22.4% (average 14.2%) (Table 1). The difference of HHI among the Es3 and Es4 source rock extracts is much less dramatic with an average value of 7.0% and 8.0%, respectively. Interestingly, a nearly linear correlation between C₃₂H/C₃₁H ratio and HHI was observed for the studied samples (Fig. 4A). Gammacerane is present in very different concentrations in the studied samples. The gammacerane index, calculated as the ratio of gammacerane to C₃₀ hopane (G/C₃₀H), varies between 0.04 and 0.48 in the Es3 oil samples and from 0.63 to 1.1 in the Es4 oils (Table 1). Lower

G/C₃₀H values were also observed for the Es3 bitumens compared to the Es4 source rocks. Positive correlation between C₃₂H/C₃₁H and G/C₃₀H ratios is obvious with correlation coefficients of 0.66 and 0.69 for the Es3 and Es4 oils, respectively (Fig. 4B).

Most samples in the present study have phytane concentrations higher than pristane and the Pr/Ph ratio varies from 0.14 to 1.14 in all studied samples. The average Pr/Ph ratios of the Es3 and Es4 oils are 0.55 and 0.25, respectively, while slightly higher values of Pr/Ph were observed for bitumens with an average value of 0.59 and 0.56 for the Es3 and Es4 source rocks, respectively (Table 1). Overall low Pr/Ph ratios suggest that Shahejie Formation source rocks formed under reducing depositional environments. A general negative correlation between C₃₂H/C₃₁H and Pr/Ph ratios occurs in the studied sample suite (Fig. 4C). Good correlation between C₃₂H/C₃₁H and those well-established redox sensitive parameters implies that the C₃₂H/C₃₁H ratio can serve as another geochemical proxy for the depositional redox condition assessment.

4.2. Maturity impact on terpane related parameters

Measured vitrinite reflectance (%Ro) values in core samples from well NY1 are in the range of 0.44–0.67%, and those from well NY1 and LY1 are 0.48–0.76% and 0.52–0.86% (Fig. 5A) [30–31]. While the exact value of %Ro might be suppressed due to the nature of lacustrine Type I kerogen [29], molecular ratios such as Ts/(Ts + Tm) and the ratio of tricyclic terpanes to pentacyclic terpanes (TT/PT) show good correlations with vitrinite reflectance in the studied wells. The TT/PT ratio values in well NY1 vary from 0.01 to 0.35, while those from well LY1 increase from 0.1 at 3580 m to 1.14 at 3830 m (Fig. 5B). Depth profiles of Ts/(Ts + Tm) from wells NY1 and LY1 have been plotted in Fig. 5C, and this parameter increases from about 0.4 at 3300 m in well NY1 to greater than 0.95 at 3800 m in well LY1. While the organic input and redox conditions have inevitably exerted some influence on TT/PT and Ts/(Ts + Tm) ratios in lacustrine source rocks, good correlation with %Ro and depth suggests that thermal maturity plays the dominant role on the variety of these ratios. The Ts/(Ts + Tm) ratios from the Es3 and Es4 oils are very similar within a range of 0.33–0.54 and 0.30–0.51, respectively. Similarly, all oils have TT/PT ratios below 0.15. Relatively low Ts/(Ts + Tm) and TT/PT ratios suggest generally low maturity of oil in the Dongying Depression.

Here the TT/PT ratio has been applied as a maturity determinant for oils, because vitrinite reflectance cannot be directly measured. A plot of TT/PT and C₃₂H/C₃₁H shows no correlation for the studied oils. However, elevated TT/PT ratios correspond to low C₃₂H/C₃₁H ratios in the bitumen samples, especially the Es4 source rocks, indicating preferential cracking of high molecular-weight homohopanes (Fig. 6A). The correlation between TT/PT ratio and HHI is also very weak. An issue for HHI is that no reliable C₃₅ homohopane can be detected from some Es4 bitumens due to high maturity (Fig. 6B). Extensive cracking of homohopanes at high maturity makes HHI unusable as a redox indicator in mature source rocks. There is no obvious correlations between TT/PT and G/C₃₀H ratios in all oils and Es3 source rock extracts. However, the Es4 source rock extracts fall in two categories. Some samples have high G/C₃₀H ratios but low TT/PT ratios, reflecting hypersaline conditions, while others show linear correlation between G/C₃₀H and TT/PT ratios, suggesting maturity related variation due to preferential cracking of C₃₀H (Fig. 6C).

5. Discussion

5.1. Why the C₃₂H/C₃₁H ratio is needed

Redox conditions are known to affect the distribution of terpanes [8]. Our data from the Dongying Depression illustrate that high values of C₃₂H/C₃₁H correspond with high values of HHI and G/C₃₀H, suggesting that C₃₂H/C₃₁H is sensitive to depositional environment as well. However, HHI and gammacerane index have been applied as depositional environment indicators for decades, why the C₃₂H/C₃₁H ratio is needed. Our first concern is maturity sensitivity. The thermal maturity influence on HHI is a well-documented phenomenon. In our studied samples, no C₃₄ and C₃₅ homohopanes can be reliably detected in the Es4 bitumens when Ro > 0.75% in well LY1, which limits the utility of HHI as redox indicator. The decrease of HHI with increasing thermal maturity has also been reported in related mature oils [8, 34]. While maturity influence on C₃₂H/C₃₁H has not been systematically documented, the correlation between C₃₂H/C₃₁H and TT/PT ratios in our studied samples suggests that C₃₂H/C₃₁H ratio suffers similar influence as the C₃₅H/C₃₄H ratio but much less dramatically. HHI was deteriorated at early oil generation stage and no reliable HHI can be obtained from source rocks Ro ≥ 0.75%, while reliable C₃₂H/C₃₁H ratio can be calculated up to Ro ≤ 1.0% when regular hopanes are largely vanished and the C₃₂H/C₃₁H ratio remains valid until Ro ≤ 0.85% in the Dongying Depression. Pan et al. [35] documented the results of pyrolysis experiments performed on a source rock (YHS1) deposited in a saline environment. The samples were heated to temperatures of 180, 210, 240, 270, 300, and 320°C during 2 h and isothermally hold for 72 h in a confined system (Au capsules) under 50 MPa. The original sample shows obvious elevated C₃₂ and C₃₅ homohopanes with C₃₅H/C₃₄H and C₃₂H/C₃₁H ratios of 1.29 and 1.12, respectively. Once heated to 180°C, the C₃₅H/C₃₄H and C₃₂H/C₃₁H ratios drop to 0.93 and 0.99, respectively, with 28% and 12% of reduction. The C₃₅H/C₃₄H and C₃₂H/C₃₁H ratios in pyrolysates at 320°C are 0.89 and 0.82, a 31% and 26% of reduction. Hydrous pyrolysis experiments performed by Peters and Moldowan [8] for Monterey shale delivered the similar results. The unheated siliceous member (GC-MS No. 767) has C₃₁ to C₃₅ homohopanes in relative percentage of 30.8, 25.2, 17.3, 8 and 18.7, respectively. Once heated at 290°C, relative percentage of C₃₁ to C₃₅ homohopanes becomes 38.9, 27.1, 17.6, 8.2 and 8.2, respectively. The C₃₂H/C₃₁H ratio drops from 0.82 to 0.7 with 14.5% of reduction, while the HHI and C₃₅H/C₃₄H ratios drop from 18.7 to 8.2 and from 2.3 to 1.0, with 56.1% and 57.2% of reduction. The pyrolysis results are consistent with our observations for the Es4 source rocks where no reliable HHI can be obtained when TT/PT ratios are > 0.4 and C₃₂H/C₃₁H ratios decrease accordingly with increasing TT/PT ratios. However, much slow reduction of C₃₂H/C₃₁H ratio as compared to HHI and C₃₅H/C₃₄H ratios attests a wider valid range of C₃₂H/C₃₁H ratio during maturation.

High gammacerane abundance is a strong indicator of hypersalinity and/or water column stratification during deposition of sediments [7, 36]. Gammacerane mainly originates from tetrahymanol in bacterivorous ciliates living in hypersaline water [37]. High G/C₃₀H ratios in the Es4 source rocks and related oils (Table 1) reflect salinity stratification and are a marker for photic zone anoxia during source rock deposition, which is supported by the high sulfur content of the Es4 oils [25]. Low gammacerane index values (G/C₃₀H generally < 0.4) in the Es3 source rocks and related oils indicate no stratified water or very low

salinity in the palaeolake during the deposition of sediments. However, gammacerane is thermally more stable than C₃₀ hopane. Once hopane thermal cracking was initiated, gammacerane index increases linearly with maturity (Fig. 6). Zhang et al. [38] noted that some abnormally high gammacerane indexes in source rock bitumen might be caused by preferential cracking of C₃₀H and cannot be regarded as a proxy for depositional environment in the Dongying Depression. While maturity inevitably affects relative abundance of C₃₁ and C₃₂ homohopanes, thermal stability difference between them is less significant than the difference between C₃₀H and gammacerane [11], which makes validity range of the C₃₂H/C₃₁H ratio less sensitive to maturation than the G/C₃₀H ratio.

The second consideration is biodegradation influence. Homohopane distributions can be altered by biodegradation. Peters et al. [39] demonstrated that biodegradation can result in selective loss of low molecular weight homologs, while C₃₅ homohopanes are more resistant. The HHI increase dramatically with the extent of biodegradation because C₃₅ homohopanes are demethylated less readily than their lower homologs. Similarly, gammacerane has much higher biodegradation resistivity than other regular hopanes and becomes the dominant component in the m/z 191 mass chromatograms of heavily biodegraded oils [40]. While heavily biodegraded oils have not been selected in the present study, selective preservation of C₃₅ homohopanes and gammacerane have been noted from biodegraded oils in the Dongying Depression [32]. However, biodegradation preference between C₃₁ and C₃₂ homohopanes is much less distinctive compared to compounds in the HHI and G/C₃₀H. Therefore, the C₃₂H/C₃₁H ratio is more robust than HHI and G/C₃₀H in biodegraded oils.

The third advantage to use the C₃₂H/C₃₁H ratio is its sensitivity in redox conditions. High C₃₅-homohopane indices are typical of marine, low Eh environments of deposition. The elevated C₃₅-homohopanes for the lacustrine oil indicate a highly reducing source rock depositional environment, most likely related to hypersalinity during the deposition. However, in anoxic, freshwater lacustrine environments, this enhanced preservation of higher hopane homologs does not occur, probably because the appropriate mechanism for sulfur incorporation is not operative [8]. Therefore, low C₃₅-homohopane index does not imply the oxic depositional system. Similarly, high gammacerane index may reflect hypersaline and strong reducing conditions in lacustrine depositional system, but low gammacerane index does not necessarily reflect oxic conditions. On other hand, the C₃₂H/C₃₁H ratio can differentiate reducing from oxic depositional environments in a similar manner as Pr/Ph ratio. The Pr/Ph ratio is one of the most commonly used geochemical parameters and has been widely invoked as an indicator of redox conditions in the depositional environment and source of organic matter [2]. Organic matter derived from terrigenous plants would be expected to have high Pr/Ph ratios of > 3.0 (oxic conditions), while organic matter formed under anoxic conditions normally has low Pr/Ph ratios of < 1.0 [2]. High C₃₂H/C₃₁H ratio (> 0.8) indicates reducing conditions, while low C₃₂H/C₃₁H ratio (< 0.8) reflects oxic conditions and extremely low C₃₂H/C₃₁H ratio (< 0.4) is indicative of coal (see further discussion in next section).

5.2. Does C₃₂H/C₃₁H ratio work for other petroleum systems

The geochemical significance of the C₃₂H/C₃₁H ratio as a redox proxy needs more supportive data from different environments. Here are a few case histories documented in the literature. Pan et al. [35] reported six Oligocene lacustrine source rock samples from the Qaidam Basin, NW China. Those samples are formed under sulfidic conditions in the Ganchaigou Formation and are thermally immature near the oil generation threshold. Pan et al. [35] found that C₃₁-C₃₅ homohopanes show unusual distribution patterns. In addition to high C₃₅H/C₃₄H ratios ranging from 1.27 to 3.42 (average 1.91), five samples have the C₃₂H/C₃₁H ratios above the unit with the highest value of 1.69 (average 1.31). The co-variation of the C₃₂H/C₃₁H and C₃₅H/C₃₄H ratios provides supportive evidence that elevated C₃₂H/C₃₁H ratio (> 1.0) can reflect highly reducing environment (Fig. 7A). Gülbay and Korkmaz [41] documented the Tertiary immature oil shale deposits in NW Anatolia, Turkey. The Miocene Beypazarı oil shale is unconformably set above the Paleocene-Eocene red-colored clastic deposits and interbedded with lignite. The Oligocene Bahçecik oil shale consists of marl, shale and tuff. Himmetoğlu and Gölpaazarı oil shales are normal clastic deposits formed in the Paleocene-Eocene and Oligocene, respectively. Those oil shales are typically characterized by high hydrogen index and low oxygen index values. The relationship among HHI, G/C₃₀H and C₃₂H/C₃₁H explored here may further clarify the reducing intensity. Both C₃₃ and C₃₄ homohopanes are absent in the Himmetoğlu and Gölpaazarı oil shales but C₃₅ homohopanes were well preserved, whereas no C₃₅ homohopanes can be detected from the Beypazarı oil shale and the C₃₅ homohopanes are lower than C₃₄ homohopanes in the Bahçecik oil shale (Fig. 7B). The G/C₃₀H ratios in the Himmetoğlu and Gölpaazarı oil shales are 0.32 and 0.31, while values for the Beypazarı and Bahçecik oil shales are 0.13 and 0.08, respectively. The C₃₂H/C₃₁H ratios in the Himmetoğlu and Gölpaazarı oil shales are 1.80 and 0.81, while values for the Beypazarı and Bahçecik oil shales are 0.74 and 0.42, respectively. All HHI, G/C₃₀H and C₃₂H/C₃₁H values suggest that Himmetoğlu and Gölpaazarı oil shales were formed under stronger reducing environment than Beypazarı and Bahçecik oil shales.

Peters and Moldowan [8] reported a suite of Monterey oils from offshore California. The Monterey Formation was deposited in silled marine basins under highly reducing conditions without hypersalinity. The gammacerane occurs in very low abundance in these oils. The C₃₅H/C₃₄H ratios in all oils are > 1.0, whereas the C₃₂H/C₃₁H ratios are in the range of 0.88 to 1.08 (average 0.95). Only one low mature sample (#549 in original paper) out of nine studied oils has C₃₂H/C₃₁H ratio > 1.0 (Fig. 7C). Data from the Monterey oils may suggest that hypersalinity likely facilitates the preservation of C₃₂ homohopanes, although maturity interference with the distribution of homohopanes cannot be ruled out.

ten Haven et al. [42] studied the Messinian marl (late Miocene) formed in an evaporitic basin from Utah, USA. All samples have very low Pr/Ph ratios (< 0.1), high abundance of gammacerane, and extended hopanes maximizing at C₃₅, indicating hypersaline environments. While no relative abundance of homohopanes has been mentioned in the original paper, elevated C₃₂ homohopanes with C₃₂H/C₃₁H ratio > 1.0 was illustrated in the m/z 191 mass chromatograms for the Rozel Point oil (Fig. 2 in ten Haven et al. [42]). Mello et al. [9] studied a wide range oils from the major Brazilian offshore basins. Group III oils are characterized by a slight even/odd preference of *n*-alkanes, the predominance of phytane over pristane, high concentration of gammacerane, and C₃₅H/C₃₄H ≥ 1.0. Inferred depositional environment for the source rock of this oil group is marine evaporitic under hypersaline conditions. Again, no C₃₂H/C₃₁H ratio has been measured in the original paper, but the m/z 191 mass chromatograms for Group III oils show similar abundance of C₃₁ and C₃₂ homohopanes (Fig. 5 in Mello et al. [9]).

On the other hand, samples from typical oxic depositional environments have very low $C_{32}H/C_{31}H$ ratio. Peters and Molddowan [8] used the Brac and Famoso bitumens derived from oxic carbonate sediments as comparison for HHI variation. Their $C_{35}H/C_{34}H$ ratios are 0.50 and 0.65, respectively, and $C_{32}H/C_{31}H$ ratios are 0.46 and 0.71, respectively (Fig. 7D). Both $C_{35}H/C_{34}H$ and $C_{32}H/C_{31}H$ ratios are systematically lower than these formed under highly reducing conditions. Wang [17] recorded anomalous hopane distributions in marine sediments of the Meishan section at the Permian–Triassic boundary. While no full homohopane distribution has been documented, the $C_{32}H/C_{31}H$ ratios in 67 samples ranging from 0.38 to 0.72 (average 0.57), showing typical feature of coals and soils. These hopanes were originated from acidified soil and peat and signified the end-Permian mass extinctions and marine ecosystem collapse [17]. A coal from early Eocene in the Fushun Basin, North China has been illustrated in Fig. 7D for the comparison purpose. It is a low maturity coal with vitrinite reflectance about 0.5%. The C_{31} homohopanes account for 82% of extended hopanes and the $C_{32}H/C_{31}H$ ratio is only 0.15. The unusual enrichment of C_{31} -homohopanes results in extremely low $C_{32}H/C_{31}H$ ratio (< 0.4) is a defined terrigenous organic matter, especially in coals and soils under strong oxic conditions.

A plot of $C_{32}H/C_{31}H$ ratio vs. HHI using above mentioned case studies shows positive correlation, indicating that both parameters can be applied for redox condition assessment (Fig. 7E). Limited data in the present study (Fig. 4A), coupled with these published in literature, show a clear boundary between strong reducing and suboxic conditions at $C_{32}H/C_{31}H$ ratio of 0.8, whereas a boundary of redox conditions is difficult to define on the base of HHI.

5.3. Mechanisms for the $C_{32}H/C_{31}H$ ratio as a redox proxy

Preferential preservation of C_{35} homohopanes was attributed to the incorporation of sulfur into the bacteriohopanoid side chain during diagenesis, which mainly occurs in marine sediments formed under anoxic depositional conditions [14]. Abnormally high HHI encountered in lacustrine saline/hypersaline sediments [21], such as the Es4 source rocks and related oils, may share the same mechanism as the marine one, where sulfurization prevails in the organic-rich source rocks. However, this enhanced preservation of C_{35} homohopanes does not occur in freshwater sediments deposited under oxic or suboxic conditions. A narrower carbon number range of homohopane distributions commonly ranging from C_{31} to C_{33} and relatively lower HHI as illustrated by the Es3 petroleum system indicate unique freshwater bacterial and/or terrigenous organic matter input.

The mechanisms for the $C_{32}H/C_{31}H$ ratio as a redox proxy are generally similar to HHI but operate in slightly different ways. The availability of free oxygen during deposition likely plays the dominant role on the $C_{32}H/C_{31}H$ ratio variation. As homohopanes are mainly derived from bacteriohopanetetrols, diagenetic and catagenetic alteration during burial result in complex reactions including sulfurization, cyclization, side chain cleavage and condensation [15]. Farrimond et al. [12] revealed that both Priest Pot (freshwater lake) and Framvaren Fjord (sulfidic) samples released high amounts of C_{32} and C_{35} bound homohopanes by hydrolysis from kerogen, but the relative abundance of C_{35} homohopanes is much higher for samples from Framvaren Fjord than from Priest Pot. The C_{30} and C_{35} are biohopanoids incorporated into the kerogen, while C_{32} hopanoic acids and hopanols are the main diagenetic products. The C_{31} , C_{33} , and C_{34} are likely derived by side-chain cleavage of higher molecular weight bound hopanoids (C_{35} and/or C_{32}) during the hydrolysis procedure [12]. Richnow et al. [43] noted that oxygen-linked hopanoids showed a greater proportion of side-chain shortened homologues, which is consistent with early diagenetic products that had become incorporated into the macromolecular structure. Thiel et al. [44] found high concentrations of free C_{32} bis-homohopanoic acids occur in microbial mats at methane seeps in anoxic Black Sea waters. The carboxyl group might be reduced to C_{32} -homohopanes under anoxic conditions, otherwise, the C_{32} acid would be oxidized to C_{31} -homohopane if free oxygen was available [8]. Therefore, the $C_{32}H/C_{31}H$ ratio ultimately preserved in organic matter and related oil may be sensitive to oxic vs. anoxic conditions.

6. Conclusions

Source rocks of the Eocene Shahejie Formation in the Dongying Depression originated from a range of depositional environments. The fourth member (Es4) formed under highly reducing, sulfidic and stratified hypersaline water. The bitumen and oil derived from Es4 are characterized by high abundances of gammacerane, C_{35} homohopanes, and low Pr/Ph (< 0.5). The third member (Es3) formed under dysoxic, brackish to freshwater with relatively more higher-plant input and/or bacterially reworked organic matter. Bitumen and oil from the Es3 member show distinct opposite features compared to the Es4 counterpart.

The $C_{32}H/C_{31}H$ ratios are linearly correlated to homohopane index (HHI), gammacerane index ($G/C_{30}H$) and Pr/Ph ratios, suggesting that $C_{32}H/C_{31}H$ can serve as a novel depositional environment proxy. High $C_{32}H/C_{31}H$ ratios (> 0.8) may indicate sulfidic, anoxic hypersaline conditions, while low ratios (< 0.8) reflect sub-oxic to oxic conditions in brackish to freshwater.

The mechanisms governing $C_{32}H/C_{31}H$ variation are like those for HHI, $G/C_{30}H$ and Pr/Ph but operate in slightly different ways. The availability of free oxygen during deposition likely plays a dominant role on variation of the $C_{32}H/C_{31}H$ ratio. When free oxygen is available under oxic or suboxic conditions, the precursor bacteriohopanetetrol is oxidized to a C_{32} acid, followed by loss of the carboxyl group to form the C_{31} homohopane or, if oxygen is depleted, the C_{32} homolog is preserved.

While the $C_{32}H/C_{31}H$ ratio can be influenced by secondary alteration, it is not only much more robust than HHI and gammacerane index during thermal maturation and biodegradation, but also more sensitive to differentiate reducing from oxic conditions.

7. Declarations

Author Contribution statement

C.j. and H.H. wrote the main manuscript text. Z.L. and Z.Z. collected samples and performed laboratory analysis. H.Z. prepared the figure. All authors reviewed the manuscript.

Competing interests

The authors declare no competing non-financial/financial interests.

Acknowledgments

This work was supported by National Natural Science Foundation of China (grant number 41873049) and Sinopec Shengli Oilfield. Prof. Steve Larter, Prof. Ken Peters and Dr. Joseph Curiale are gratefully acknowledged for their valuable suggestions and comments that substantially improved the quality of the manuscript.

8. References

1. Bray, E. E. & Evans, E. D. Distribution of n-paraffins as a clue to recognition of source beds. *Geochim Cosmochim Acta*. **22**, 2–15 (1961).
2. Didyk, B., Simoneit, B., Brassell, S. C. & Eglinton, G. Organic geochemical indicators of palaeoenvironmental conditions of sedimentation. *Nature*. **272**, 216–222 (1978).
3. Huang, Y. & Meinschein, W. G. Sterols as ecological indicators. *Geochim Cosmochim Acta*. **43**, 739–745 (1979).
4. Noble, R. A., Alexander, R., Kagi, R. I. & Knox, J. Identification of some diterpenoid hydrocarbons in petroleum. *Org Geochem*. **10**, 825–829 (1985).
5. Holba, A. G. *et al.* Application of tetracyclic polyprenoids as indicators of input from fresh–brackish water environments. *Org Geochem*. **34**, 441–469 (2003).
6. Moldowan, J. M., Seifert, W. K. & Gallegos, E. J. Relationship between petroleum composition and depositional environment of petroleum source rocks. *AAPG Bull.* **69**, 1255–1268 (1985).
7. Moldowan, J. M., Sundararaman, P. & Schoell, M. Sensitivity of biomarker properties to depositional environment and/or source input in the Lower Toarcian of S.W. Germany. *Org Geochem*. **10**, 915–926 (1986).
8. Peters, K. E. & Moldowan, J. M. Effects of source, thermal maturity and biodegradation on the distribution and isomerization of homohopanes in petroleum. *Org Geochem*. **17**, 47–61 (1991).
9. Mello, M. R., Gaglianone, P. C., Brassell, S. C. & Maxwell, J. R. Geochemical and biological marker assessment of depositional environments using Brazilian offshore oils. *Mar Pet Geol*. **5**, 205–223 (1988).
10. Ourisson, G., Albrecht, P. & Rohmer, M. The hopanoids, palaeochemistry and biochemistry of a group of natural products. *Pure Appl Chem*. **51**, 709–729 (1979).
11. Farrimond, P., Taylor, A. & Telnaés, N. Biomarker maturity parameters, the role of generation and thermal degradation. *Org Geochem*. **29**, 1181–1197 (1998).
12. Farrimond, P. *et al.* Evidence for the rapid incorporation of hopanoids into kerogen. *Geochim Cosmochim Acta*. **67**, 1383–1394 (2003).
13. Clark, J. P. & Philp, R. P. Geochemical characterization of evaporate and carbonate depositional environments and correlation of associated crude oils in the Black Creek Basin, Alberta. *Bull Can Pet Geol*. **37**, 401–416 (1989).
14. Sinninghe Damsté, J. S., Van Duin, A. C. T., Hollander, D., Kohnen, M. E. L. & de Leeuw, J. W. Early diagenesis of bacteriohopanepolyol derivatives, Formation of fossil homohopane derivatives. *Geochim Cosmochim Acta*. **59**, 5141–5157 (1995).
15. Köster, J., Van Kaam–Peters, H. M., Koopmans, M. P., de Leeuw, J. W. & Sinninghe Damsté, J. S. Sulfurization of homohopane derivatives, Effects on carbon number distribution, speciation, and 22S/22R epimer ratios. *Geochim Cosmochim Acta*. **61**, 2431–2452 (1997).
16. French, K. L., Tosca, N. J., Cao, C. & Summons, R. E. Diagenetic and detrital origin of moretane anomalies through the Permian–Triassic boundary. *Geochim Cosmochim Acta*. **84**, 104–125 (2012).
17. Wang, C. Anomalous hopane distributions at the Permian–Triassic boundary, Meishan, China—evidence for the end–Permian marine ecosystem collapse. *Org Geochem*. **38**, 52–66 (2007).
18. Lerch, B., Karlsen, D. A. & Seland, R. & Backer–Owe, K. Depositional environment and age determination of oils and condensates from the Barents Sea. *Pet Geosci*. **23**, 190–209 (2017).
19. Bishop, A. N. & Farrimond, P. A new method of comparing extended hopane distributions. *Org Geochem*. **23**, 987–990 (1995).
20. Philp, R. P., Jinggui, L. & Lewis, C. A. An organic geochemical investigation of crude oils from Shangganning, Jiangnan, Chaidamu and Zhungeer basins, People's Republic of China. *Org Geochem*. **14**, 447–460 (1989).
21. Fu, J. M. *et al.* Application of biological markers in the assessment of paleoenvironments of Chinese non–marine sediments. *Org Geochem*. **16**, 769–779 (1990).
22. Moldowan, J. M. *et al.* Source correlation and maturity assessment of select oils and rocks from the Central Adriatic Basin (Italy and Yugoslavia). In J.M. Moldowan (eds.) *Biological Markers in Sediments and Petroleum*. Prentice–Hall, p. 370–401(1992).
23. Li, S., Pang, X., Li, M. & Jin, Z. Geochemistry of petroleum systems in the Niuzhuang South Slope of Bohai Bay Basin—Part 1, source rock characterization. *Org Geochem*. **34**, 389–412 (2003).

24. Zhang, L., Liu, Q., Zhu, R., Li, Z. & Lu, X. Source rocks in Mesozoic–Cenozoic continental rift basins, East China, a case from Dongying Depression, Bohai Bay Basin. *Org Geochem.* **40**, 229–242 (2009).
25. Zhan, Z. *et al.* Chemometric differentiation of crude oil families in the southern Dongying Depression, Bohai Bay Basin, China. *Org Geochem.* **127**, 37–49 (2019).
26. Wang, Q. & Huang, H. Perylene preservation in an oxidizing paleoenvironment and its limitation as a redox proxy. *Palaeogeogr Palaeoclimatol Palaeoecol.* **562**, 110104 (2021).
27. Allen, M. B., Macdonald, D. I. M., Xun, Z., Vincent, S. J. & Brouet–Menziés, C. Early Cenozoic two–phase extension and late Cenozoic thermal subsidence and inversion of the Bohai Basin, northern China. *Mar Pet Geol.* **14**, 951–972 (1997).
28. Lampe, C., Song, G., Cong, L. & Mu, X. Fault control on hydrocarbon migration and accumulation in the Tertiary Dongying Depression, Bohai Basin, China. *AAPG Bull.* **96**, 983–1000 (2012).
29. Guo, X. *et al.* Petroleum generation and charge history of the northern Dongying Depression, Bohai Bay Basin, China, insight from integrated fluid inclusion analysis and basin modelling. *Mar Pet Geol.* **32**, 21–35 (2012).
30. Ping, H., Chen, H., George, S. C., Li, C. & Hu, S. Relationship between the fluorescence colour of oil inclusions and thermal maturity in the Dongying Depression, Bohai Bay Basin, China, Part 2. Fluorescence evolution of oil in the context of petroleum generation, expulsion and cracking under geological conditions. *Mar Pet Geol.* **103**, 306–319 (2019).
31. Zhang, H., Huang, H., Li, Z. & Liu, M. Oil physical status in lacustrine shale reservoirs–A case study on Eocene Shahejie Formation shales, Dongying Depression, East China. *Fuel.* **257**, 116027 (2019).
32. Wang, G., Wang, T. G., Simoneit, B. R. & Zhang, L. Investigation of hydrocarbon biodegradation from a downhole profile in Bohai Bay Basin: Implications for the origin of 25–norhopanes. *Org Geochem.* **55**, 72–84 (2013).
33. Bastow, T. P., van Aarssen, B. G. K. & Lang, D. Rapid small–scale separation of saturate, aromatic and polar components in petroleum. *Org Geochem.* **38**, 1235–1250 (2007).
34. Vu, T. T. A. *et al.* Changes in bulk properties and molecular compositions within New Zealand Coal Band solvent extracts from early diagenetic to catagenetic maturity levels. *Org Geochem.* **40**, 963–977 (2009).
35. Pan, C. *et al.* Distribution and isomerization of C31–C35 homohopanes and C29 steranes in Oligocene saline lacustrine sediments from Qaidam Basin, Northwest China. *Org Geochem.* **39**, 646–657 (2008).
36. Sinninghe Damsté, J. *et al.* Evidence for gammacerane as an indicator of water column stratification. *Geochim Cosmochim Acta.* **59**, 1895–1900 (1995).
37. ten Haven, H. L., Rohmer, M., Rullkötter, J. & Bissere, P. Tetrahymanol, the most likely precursor of gammacerane, occurs ubiquitously in marine sediments. *Geochim Cosmochim Acta.* **53**, 3073–3079 (1989).
38. Zhang, H., Huang, H., Li, Z. & Liu, M. Impact of maturation on the validity of paleo–environmental indicators, Implication for discrimination of oil genetic types in lacustrine shale systems. *Energy & Fuels.* **34**, 6962–6973 (2020).
39. Peters, K. E., Moldowan, J. M., McCaffrey, M. A. & Fago, F. J. Selective biodegradation of extended hopanes to 25–norhopanes in petroleum reservoirs. Insights from molecular mechanics. *Org Geochem.* **24**, 765–783 (1996).
40. Huang, H. & Li, J. Molecular composition assessment of biodegradation influence at extreme levels–a case study from oilsand bitumen in the Junggar Basin, NW China. *Org Geochem.* **103**, 31–42 (2017).
41. Gülbay, R. K. & Korkmaz, S. *Org Geochem*, depositional environment and hydrocarbon potential of the tertiary oil shale deposits in NW Anatolia, Turkey. *Oil Shale.* **25**, 444–464 (2008).
42. ten Haven, H. L. *et al.* Application of biological markers in the recognition of palaeohypersaline environments. *Geological Society, London, Special Publications.* **40**, 123–130 (1988).
43. Richnow, H. H., Jenisch, A. & Michaelis, W. Structural investigations of sulphur–rich macromolecular oil fractions and a kerogen by sequential chemical degradation. *Org Geochem.* **19**, 351–370 (1992).
44. Thiel, V., Blumenberg, M., Pape, T., Seifert, R. & Michaelis, W. Unexpected occurrence of hopanoids at gas seeps in the Black Sea. *Org Geochem.* **34**, 81–87 (2003).

9. Tables

Table 1

Biomarker compositions of oils and source rock extracts from the Dongying Depression

| Well | Age | Type | Depth (m KB) | Pr/Ph | C ₂₉ H/C ₃₀ H | C ₃₂ H/C ₃₁ H | HHI | C ₃₀ D/C ₂₉ Ts | G/C ₃₀ H | C ₃₁ R/C ₃₀ H | C ₂₇ St% | C ₂₈ St% | C ₂₉ St% |
|-----------|-----|------|-----------------|-------|-------------------------------------|-------------------------------------|-------|--------------------------------------|---------------------|-------------------------------------|---------------------|---------------------|---------------------|
| Jin31-1 | Es3 | oil | 1230.6-1254.7 | 0.80 | 0.56 | 0.64 | 5.08 | 0.42 | 0.06 | 0.21 | 29.5 | 30.0 | 40.5 |
| Tong61-70 | Es3 | oil | 1796.6-1799 | 0.31 | 0.45 | 0.73 | 7.85 | 0.45 | 0.32 | 0.26 | 23.9 | 27.7 | 48.3 |
| Wang3-12 | Es3 | oil | 2215-2218.2 | 0.36 | 0.44 | 0.74 | 6.93 | 0.23 | 0.28 | 0.24 | 25.8 | 28.5 | 45.7 |
| Wang631 | Es3 | oil | 2775.2-2784 | 0.49 | 0.51 | 0.59 | 2.87 | 0.28 | 0.18 | 0.26 | 29.3 | 25.7 | 45.0 |
| F15-27 | Es3 | oil | 2908.5-3000 | 1.06 | 0.51 | 0.66 | 5.58 | 0.37 | 0.04 | 0.23 | 32.1 | 28.3 | 39.6 |
| F10-X603 | Es3 | oil | 2973-2977 | 1.08 | 0.48 | 0.68 | 6.05 | 0.34 | 0.04 | 0.22 | 29.6 | 31.7 | 38.7 |
| F20-722 | Es3 | oil | 2978-2983 | 1.08 | 0.53 | 0.68 | 6.49 | 0.47 | 0.04 | 0.24 | 31.9 | 28.6 | 39.5 |
| Niu6 | Es3 | oil | 2999.2-3209.6 | 0.30 | 0.46 | 0.87 | 9.85 | 0.35 | 0.48 | 0.25 | 28.7 | 25.5 | 45.8 |
| F18-716 | Es3 | oil | 3109.5-3120 | 1.07 | 0.48 | 0.68 | 5.45 | 0.32 | 0.04 | 0.24 | 32.1 | 29.4 | 38.4 |
| Niu37-1 | Es3 | oil | 3111.2-3125.5 | 0.51 | 0.53 | 0.71 | 6.65 | 0.23 | 0.08 | 0.23 | 27.0 | 30.0 | 43.1 |
| F18-720 | Es3 | oil | 3142-3146 | 1.07 | 0.48 | 0.68 | 5.12 | 0.44 | 0.05 | 0.23 | 31.5 | 31.6 | 36.9 |
| Wang542 | Es3 | Oil | 3147.4-3162.2 | 0.50 | 0.42 | 0.68 | 3.67 | 0.33 | 0.24 | 0.24 | 23.9 | 21.4 | 54.7 |
| Niu2 | Es3 | Oil | 3190.4-3200.6 | 0.37 | 0.43 | 0.75 | 7.45 | 0.29 | 0.42 | 0.23 | 24.6 | 21.9 | 53.4 |
| Wang543 | Es3 | Oil | 3214.0-3223.0 | 0.46 | 0.43 | 0.68 | 3.78 | 0.31 | 0.23 | 0.23 | 23.6 | 21.6 | 54.8 |
| F21-720 | Es3 | oil | 3215.9-3231 | 0.96 | 0.61 | 0.65 | 5.75 | 0.28 | 0.04 | 0.21 | 32.3 | 28.2 | 39.5 |
| Niu871 | Es3 | Oil | 3240.0-3290.0 | 0.51 | 0.43 | 0.69 | 4.19 | 0.33 | 0.16 | 0.22 | 24.0 | 20.6 | 55.4 |
| Niu25-30 | Es3 | oil | 3254-3283.1 | 0.32 | 0.41 | 0.68 | 8.95 | 0.33 | 0.35 | 0.25 | 25.9 | 31.6 | 42.5 |
| Niu101 | Es3 | oil | 3279.3-3294.3 | 0.35 | 0.50 | 0.69 | 8.02 | 0.38 | 0.16 | 0.25 | 27.1 | 30.2 | 42.7 |
| Niu39 | Es3 | oil | 3279.8-3287.6 | 0.25 | 0.51 | 0.72 | 11.45 | 0.27 | 0.45 | 0.28 | 25.3 | 26.7 | 48.0 |
| Niu25-65 | Es3 | oil | 3280.6-3283.3 | 0.29 | 0.51 | 0.76 | 8.95 | 0.23 | 0.29 | 0.22 | 26.6 | 26.6 | 46.8 |
| Wang57 | Es3 | Oil | 3414-3415 | 0.49 | 0.43 | 0.68 | 4.22 | 0.29 | 0.18 | 0.26 | 26.8 | 19.8 | 53.4 |
| Wang78 | Es3 | Oil | 3424-3436.6 | 0.47 | 0.45 | 0.66 | 4.88 | 0.31 | 0.20 | 0.22 | 25.0 | 20.9 | 54.1 |
| M120-P1 | Es4 | oil | 1060-1294 | 0.20 | 0.27 | 1.01 | 16.36 | 0.33 | 0.94 | 0.21 | 28.6 | 29.0 | 42.4 |
| M12-11-31 | Es4 | oil | 1080-1104 | 0.19 | 0.33 | 0.87 | 14.35 | 0.27 | 0.81 | 0.22 | 25.6 | 28.9 | 45.6 |
| M14-13-X7 | Es4 | oil | 1159-1165 | 0.14 | 0.31 | 0.80 | 14.75 | 0.19 | 0.83 | 0.23 | 27.1 | 28.4 | 44.5 |
| M4-7-G7 | Es4 | oil | 1173-1208 | 0.17 | 0.28 | 0.78 | 13.94 | 0.12 | 0.76 | 0.24 | 27.4 | 28.0 | 44.6 |
| Wang73 | Es4 | Oil | 1285.6-1296.0 | 0.24 | 0.34 | 1.10 | 16.94 | 0.20 | 1.10 | 0.20 | 30.0 | 24.7 | 45.3 |
| M4-8-19 | Es4 | Oil | 1299.6-1355.4 | 0.27 | 0.34 | 1.01 | 15.20 | 0.22 | 1.03 | 0.21 | 28.7 | 25.0 | 46.3 |

| Well | Age | Type | Depth (m KB) | Pr/Ph | C ₂₉ H/C ₃₀ H | C ₃₂ H/C ₃₁ H | HHI | C ₃₀ D/C ₂₉ Ts | G/C ₃₀ H | C ₃₁ R/C ₃₀ H | C ₂₇ St% | C ₂₈ St% | C ₂₉ St% |
|-----------|-----|------|-----------------|-------|-------------------------------------|-------------------------------------|-------|--------------------------------------|---------------------|-------------------------------------|---------------------|---------------------|---------------------|
| Wang91-5 | Es4 | oil | 1399-1404 | 0.14 | 0.22 | 1.22 | 22.38 | 0.23 | 1.07 | 0.20 | 30.0 | 28.6 | 41.4 |
| WangX731 | Es4 | Oil | 1656.2-1661.0 | 0.24 | 0.35 | 1.06 | 13.74 | 0.22 | 1.00 | 0.19 | 31.0 | 24.3 | 44.8 |
| Wang21-X2 | Es4 | oil | 2429.5-2431.6 | 0.21 | 0.31 | 0.98 | 13.97 | 0.17 | 0.82 | 0.20 | 30.3 | 28.6 | 41.0 |
| Niu10 | Es4 | Oil | 2729.0-2743.6 | 0.31 | 0.42 | 0.85 | 11.43 | 0.28 | 0.63 | 0.24 | 25.6 | 23.2 | 51.3 |
| Wang143 | Es4 | Oil | 2795.4-2801.0 | 0.34 | 0.39 | 0.86 | 9.12 | 0.24 | 0.65 | 0.22 | 26.5 | 24.0 | 49.6 |
| Wang102 | Es4 | Oil | 2903.4-2952.0 | 0.32 | 0.32 | 1.09 | 14.64 | 0.33 | 1.05 | 0.22 | 27.9 | 23.1 | 49.0 |
| Guan103 | Es4 | Oil | 3006-3009 | 0.32 | 0.37 | 0.91 | 14.31 | 0.22 | 0.86 | 0.21 | 26.3 | 23.5 | 50.2 |
| Wang587 | Es4 | Oil | 3458.0-3462.3 | 0.38 | 0.33 | 0.87 | 7.62 | 0.41 | 0.86 | 0.24 | 27.0 | 21.1 | 51.8 |
| FY1 | Es3 | Rock | 3031.5 | 1.14 | 0.42 | 0.64 | 5.66 | 0.29 | 0.04 | 0.28 | 28.0 | 23.1 | 48.9 |
| FY1 | Es3 | Rock | 3059.92 | 0.88 | 0.44 | 0.65 | 6.01 | 0.34 | 0.04 | 0.26 | 29.2 | 23.9 | 46.9 |
| FY1 | Es3 | Rock | 3125.65 | 0.96 | 0.41 | 0.67 | 6.53 | 0.38 | 0.06 | 0.25 | 27.7 | 20.9 | 51.4 |
| FY1 | Es3 | Rock | 3170.14 | 1.07 | 0.45 | 0.65 | 4.89 | 0.34 | 0.05 | 0.21 | 28.7 | 19.4 | 51.9 |
| FY1 | Es3 | Rock | 3233.29 | 1.09 | 0.37 | 0.73 | 5.28 | 0.40 | 0.07 | 0.28 | 23.5 | 17.8 | 58.7 |
| FY1 | Es4 | Rock | 3316.23 | 0.72 | 0.32 | 0.74 | 5.34 | 0.68 | 0.15 | 0.30 | 28.1 | 23.2 | 48.7 |
| LY1 | Es3 | Rock | 3582.14 | 0.39 | 0.31 | 0.74 | 8.14 | 0.59 | 0.18 | 0.25 | 25.2 | 26.3 | 48.5 |
| LY1 | Es3 | Rock | 3582.14 | 0.39 | 0.31 | 0.73 | 7.49 | 0.59 | 0.17 | 0.25 | 24.5 | 25.8 | 49.7 |
| LY1 | Es3 | Rock | 3586.16 | 0.38 | 0.33 | 0.74 | 8.33 | 0.53 | 0.19 | 0.24 | 24.5 | 26.9 | 48.6 |
| LY1 | Es3 | Rock | 3593.01 | 0.38 | 0.34 | 0.75 | 8.10 | 0.49 | 0.19 | 0.23 | 24.5 | 26.6 | 48.9 |
| LY1 | Es3 | Rock | 3598.15 | 0.38 | 0.35 | 0.75 | 8.32 | 0.46 | 0.18 | 0.23 | 24.1 | 26.4 | 49.5 |
| LY1 | Es3 | Rock | 3601.21 | 0.39 | 0.35 | 0.74 | 7.86 | 0.47 | 0.18 | 0.24 | 24.3 | 25.4 | 50.3 |
| LY1 | Es3 | Rock | 3658.46 | 0.96 | 0.35 | 0.78 | 4.83 | 0.41 | 0.09 | 0.27 | 28.4 | 18.1 | 53.6 |
| LY1 | Es3 | Rock | 3672.38 | 0.88 | 0.34 | 0.75 | 4.98 | 0.44 | 0.10 | 0.29 | 26.0 | 17.3 | 56.7 |
| LY1 | Es3 | Rock | 3674.34 | 0.94 | 0.34 | 0.80 | 4.97 | 0.47 | 0.09 | 0.28 | 24.8 | 17.6 | 57.6 |
| LY1 | Es3 | Rock | 3674.34 | 0.95 | 0.34 | 0.79 | 5.09 | 0.47 | 0.09 | 0.29 | 24.5 | 17.0 | 58.5 |
| LY1 | Es4 | Rock | 3751.14 | 0.73 | 0.31 | 0.71 | 8.52 | 0.65 | 0.19 | 0.34 | 26.9 | 24.8 | 48.3 |
| LY1 | Es4 | Rock | 3768.15 | 0.59 | 0.31 | 0.64 | n/a | 0.80 | 0.31 | 0.42 | 28.3 | 24.2 | 47.6 |
| LY1 | Es4 | Rock | 3771.81 | 0.56 | 0.29 | 0.68 | n/a | 0.84 | 0.35 | 0.42 | 27.8 | 25.7 | 46.4 |
| LY1 | Es4 | Rock | 3786.16 | 0.50 | 0.38 | 0.58 | n/a | 1.00 | 0.57 | 0.43 | 25.0 | 24.4 | 50.5 |
| LY1 | Es4 | Rock | 3803.65 | 0.53 | 0.48 | 0.62 | n/a | 1.15 | 0.71 | 0.41 | 22.8 | 23.0 | 54.2 |
| LY1 | Es4 | Rock | 3815.76 | 0.55 | 0.52 | 0.67 | n/a | 0.97 | 0.66 | 0.51 | 23.6 | 23.1 | 53.3 |
| LY1 | Es4 | Rock | 3830.45 | 0.56 | 0.47 | n/a | n/a | 1.50 | n/a | n/a | 25.6 | 21.5 | 52.9 |
| NY1 | Es3 | Rock | 3304.1 | 0.86 | 0.49 | 0.66 | 6.43 | 0.22 | 0.06 | 0.24 | 26.5 | 18.2 | 55.3 |
| NY1 | Es4 | Rock | 3333.04 | 0.82 | 0.46 | 0.64 | 7.12 | 0.27 | 0.06 | 0.25 | 24.6 | 20.3 | 55.1 |
| NY1 | Es4 | Rock | 3372.9 | 0.42 | 0.39 | 0.65 | 6.27 | 0.27 | 0.07 | 0.26 | 28.8 | 23.3 | 47.8 |
| NY1 | Es4 | Rock | 3377.84 | 0.95 | 0.40 | 0.66 | 6.06 | 0.39 | 0.05 | 0.25 | 27.0 | 20.8 | 52.2 |
| NY1 | Es4 | Rock | 3402.73 | 0.50 | 0.41 | 0.69 | 6.69 | 0.27 | 0.19 | 0.28 | 22.5 | 19.8 | 57.7 |
| NY1 | Es4 | Rock | 3402.73 | 0.51 | 0.40 | 0.69 | 6.82 | 0.28 | 0.19 | 0.28 | 21.1 | 20.1 | 58.8 |
| NY1 | Es4 | Rock | 3438.12 | 0.46 | 0.27 | 0.92 | 16.65 | 0.22 | 0.71 | 0.28 | 27.6 | 23.1 | 49.3 |

| Well | Age | Type | Depth (m KB) | Pr/Ph | C ₂₉ H/C ₃₀ H | C ₃₂ H/C ₃₁ H | HHI | C ₃₀ D/C ₂₉ Ts | G/C ₃₀ H | C ₃₁ R/C ₃₀ H | C ₂₇ St% | C ₂₈ St% | C ₂₉ St% |
|------|-----|------|--------------|-------|-------------------------------------|-------------------------------------|-------|--------------------------------------|---------------------|-------------------------------------|---------------------|---------------------|---------------------|
| NY1 | Es4 | rock | 3461.4 | 0.41 | 0.36 | 1.13 | 9.20 | 0.34 | 1.22 | 0.16 | 26.3 | 25.4 | 48.3 |
| NY1 | Es4 | Rock | 3462.58 | 0.27 | 0.28 | 1.12 | 17.45 | 0.28 | 2.16 | 0.29 | 23.0 | 28.9 | 48.1 |
| NY1 | Es4 | rock | 3482.3 | 0.29 | 0.36 | 0.90 | 8.68 | 0.35 | 1.64 | 0.24 | 29.2 | 27.1 | 43.7 |

Figures

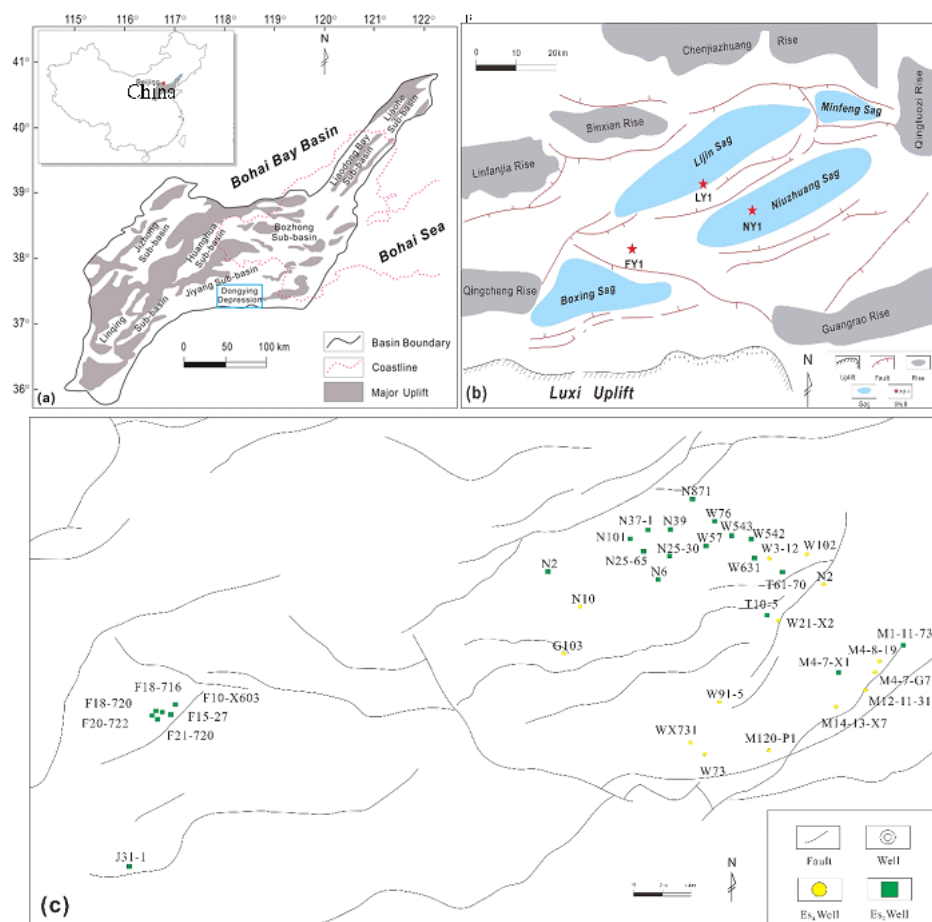


Figure 1

Location map of study area. (A) Schematic map of the Bohai Bay Basin (modified after Zhang et al., 2019); (B) Tectonic setting map of the Dongying Depression showing the uplifts, sags, main faults and core sample locations (modified after Zhang et al., 2019); (C) Oil sample locations in southern part of the Dongying Depression. Note: The designations employed and the presentation of the material on this map do not imply the expression of any opinion whatsoever on the part of Research Square concerning the legal status of any country, territory, city or area or of its authorities, or concerning the delimitation of its frontiers or boundaries. This map has been provided by the authors.

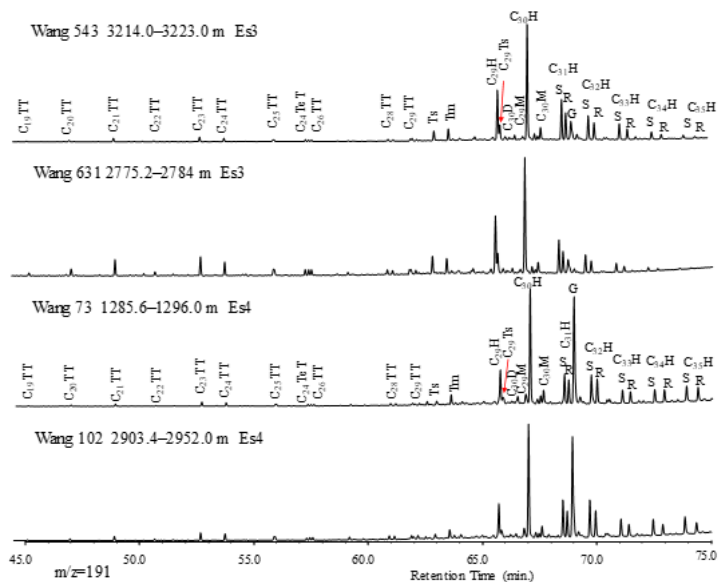


Figure 2

The $m/z = 191$ mass fragmentograms showing terpane distributions in representative oil samples from the Dongying Depression. C19-C30 TT: tricyclic terpane; Ts: 18 α (H)-trisnorhopane; Tm: 17 α (H)-trisnorhopane; C29H: C29 17 α ,21 β (H) 30-norhopane; C29Ts: C29 18 α (H)-30-norneohopane; C30D: C30 17 α (H)-diahopane; C29M: C29 17b,21a(H) 30-normoretane; C30H: C30 17 α ,21 β (H) hopane; C30M: C30 17b,21a(H) moretane; C31-C35H: C30-C35 17 α ,21 β (H) homohopane; G: gammacerane.

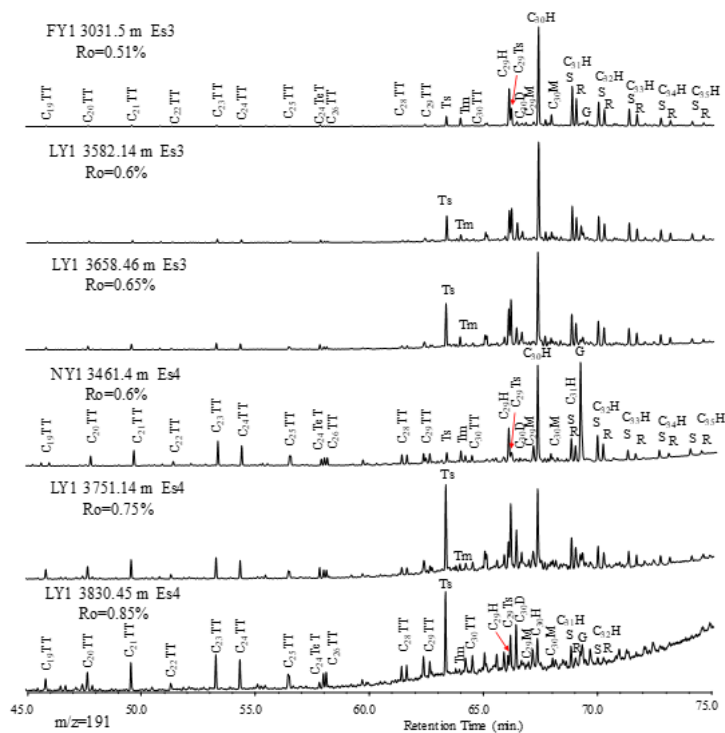


Figure 3

The $m/z = 191$ mass fragmentograms showing terpane distributions in representative bitumen samples from the Dongying Depression. Peak label refers to Fig. 2.

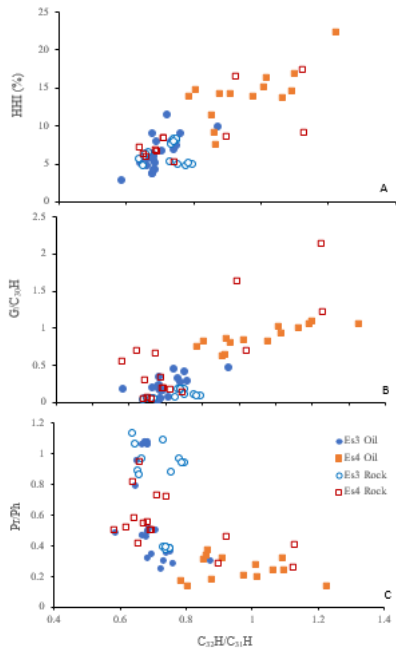


Figure 4
 Plot of C32H/C31H ratio vs. known depositional environment parameters in oil and rock samples from the Dongying Depression. (A) Homohopane index (HHI); (B) Gammacerane index (G/C30H); and (C) pristane/phytane ratio (Pr/Ph).

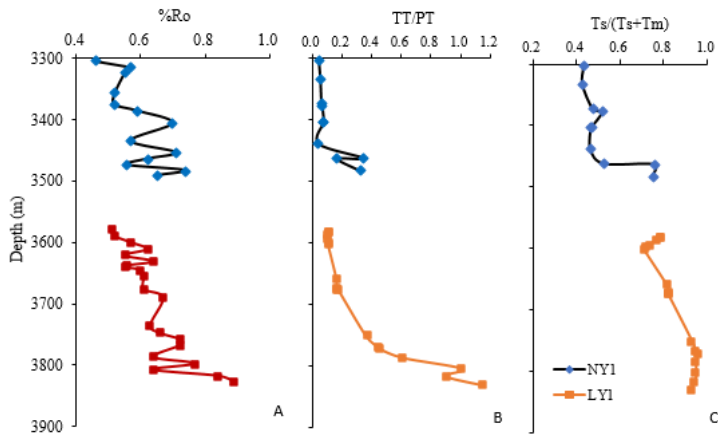


Figure 5
 Depth profile of source rock maturity in wells NY1 and LY1. (A) Measured vitrinite reflectance; (B) Concentration ratio of tri- to pentacyclic terpanes (TT/PT); (C) Concentration ratio of Ts/(Ts+Im).

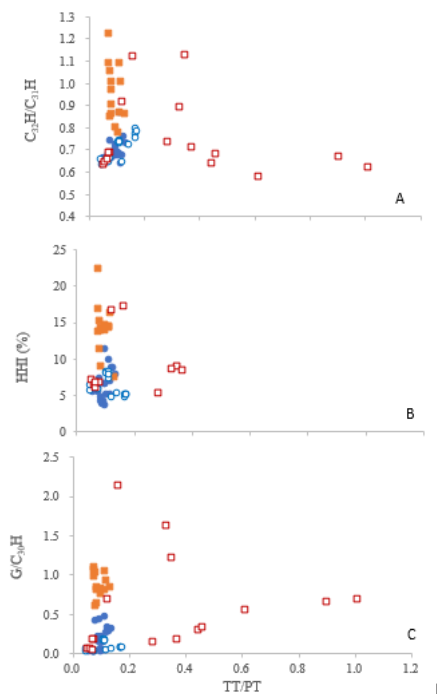


Figure 6
 Plot of TT/PT ratio with redox condition parameters in oil and rock samples from the Dongying Depression. (A) C₃₂H/C₃₁H ratio; (B) Homohopane index; (C) Gammacerane index.

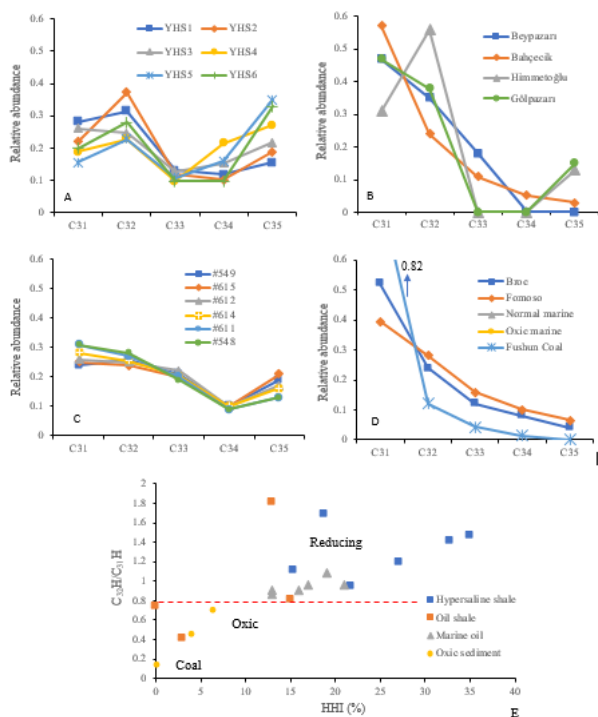


Figure 7
 Homohopane distributions for source rock and oil samples deposited under different redox conditions. (A) Tertiary saline lacustrine source rocks from the Qaidam Basin (data from Pan et al., 2008); (B) Tertiary saline oil shales in NW Anatolia, Turkey (data from Gülbay and Korkmaz, 2008); (C) Monterey oils from offshore California (data from Peters and Moldowan, 1991); (D) Oxidic carbonate and coal (data of Brac and Famoso bitumens from Peters and Moldowan, 1991). (E) Plot of HHI vs. C₃₂H/C₃₁H.